Three-dimensional finite-difference time-domain modelling of photonic crystal surface-emitting lasers

Pavlo Ivanov[1], Richard J. E. Taylor[2], Guangrui Li[2], David T. D. Childs[1], Salam Khamas[2], Jayanta Sarma[2], Robertus Erdelyi[3] and Richard A. Hogg[1]
[1]presently with the School of Engineering, Rankine building, the University of Glasgow, Glasgow, G12 8LT, UK
[2]Department of Electronic and Electrical Engineering, the University of Sheffield, Mappin street, Sheffield S1 3JD, UK
[3]School of Mathematics and Statistics, the University of Sheffield, Hicks building Hounsfield road, Sheffield, S3 7RH, UK

ABSTRACT

We investigate the beam divergence in far-field region, diffraction loss and optical confinement factors of all-semiconductor and void-semiconductor photonic-crystal surface-emitting lasers (PCSELs), containing either InGaP/GaAs or InGaP/air photonic crystals using a three-dimensional FDTD model. We explore the impact of changing the PC hole shape, size, and lattice structure in addition to the choice of all-semiconductor or void-semiconductor designs. We discuss the determination of the threshold gain from the diffraction losses, and explore limitations to direct modulation of the PCSEL.

Keywords: Photonic crystal, photonic crystal surface-emitting laser, FDTD method, photonic bands, laser waveguide

1. INTRODUCTION

Photonic crystal surface-emitting lasers (PCSELs) are semiconductor lasers with two-dimensional photonic crystals (PCs) providing both surface emission and in-plane feedback inside the laser cavity. PCSELs can generate polarization-controlled[1], low-divergent and high-power single mode laser beams[2]. It has been demonstrated that the shape of holes in the PC can control vertical optical confinement[3] and enhance the surface emission of PCSELs[4]. Recently, coherently-coupled PCSEL arrays allowing coherent power scaling[5] and electron control of coherence between elements[6] have been demonstrated.

Most PCSELs reported to date have the PC formed by a pattern of holes (atoms) sitting inside laser, which poses possible issues in reliability, manufacturability, and in flexibility of design due to the low refractive index PC layer. We therefore wished to make the device all-semiconductor and have demonstrated PCSELs with all-semiconductor $In_{0.48}Ga_{0.52}P$/GaAs PC layers through epitaxial regrowth[7]. Although semiconductor-air PCSELs have been researched extensively, all-semiconductor PCSELs are still being intensively studied.

There are two kinds of optical PCSEL models: coupled-mode-theory-based analytical models and models based on a numerical finite-difference time-domain (FDTD) method. Coupled-mode theory of PCs and PCSELs is complicated, but it also needs to be developed for each single PC geometry and polarisation[8,9,10]. Using the FDTD method, PCs and PCSELs can be modelled with minimal assumptions. Moreover, the FDTD model takes into account diffraction effects caused by the PC and waveguide effects provided by the laser waveguide. Modelled PCSELs may have any number of waveguide layers, any shape of atoms situated in any layer of the laser. However, FDTD models are very time and computer memory demanding.

In this work we use the FDTD method[11] to investigate two-dimensional PC and all-semiconductor PCSELs. We investigate the effects of PC geometry on the diffraction loss and surface emission of PCSELs. We also compare results of the FDTD method to results of an eigenmode solver were possible[12].

The PCSEL and the FDTD model will be introduced in the next two sections of the paper. The following section reports results of this work, where we present results of a convergence study of the method, and compare results of the eigenmode solver and FDTD method applied to a bulk two-dimensional PC, PC layer and PCSEL. We go on to study the effect of the PC geometry on the diffraction loss and surface emission of the PCSEL.

2. THE MODELLED LASER

The all-semiconductor PCSEL[7] emitting at ~980 nm is investigated in this work. The PCSEL structure has a single PC layer situated between the top contact layer and a quantum-well active zone as shown in the Fig. 1. The incorporation of the PC layer into the laser allows placing the PC layer closer to the laser waveguide, increasing the interaction between guided optical waves and the PC, whilst keeping the active zone (i.e. the light generating and amplifying intrinsic region) unaffected by the PC fabrication process. The PC provides two effects: in-plane feedback and diffraction resulting in surface emission. These effects are caused by the two-dimensional periodic variation of the refractive index created by photonic atoms arranged in a square crystal lattice. Compared to a DFB laser, operation of a PCSEL relies on a two-dimensional feedback that makes two-dimensional coherently-coupled PCSEL arrays possible[5,6].

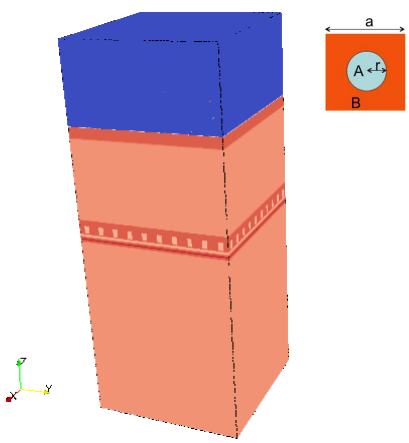

Figure 1. Schematics of a PCSEL. Inset shows a unit cell of the PC. In this work, atom's material A in PC type I is air, type II – GaAs. Material B in both PC types is InGaP.

Details of epitaxial PCSEL structure can be found elsewhere[7], but the PC needs an additional introduction. The PC layer is 150 nm thick. It contains a two-dimensional PC made of cylinders (photonic atoms) arranged into a square (photonic crystal) lattice. The PC period is a = 286 nm and the atom radius is r. These atoms sit in p-$In_{0.48}Ga_{0.52}P$ and they can be either left unfilled, i.e. semiconductor-void, (PC type I) or be filled with p-GaAs (PC type II). The all-semiconductor InGaP/GaAs PC with in-filled atoms has been applied in PCSELs[7]. However, the semiconductor-air PC has a higher refractive index contrast and can be beneficial for achieving high in-plane feedback. Thus, we consider both all-semiconductor and semiconductor-air PCs in this work.

3. THE MODEL

An electromagnetic wave propagating in a PCSEL waveguide interacts with the periodic perturbation defined by the refractive index variation in the two-dimensional PC. This interaction results in both diffraction and feedback effects that can be simulated using three-dimensional Maxwell solvers[11,12] and coupled-mode models[8,9,10]. A simplified and compact quasi-three-dimensional model of a PCSEL waveguide including diffraction and feedback effects (resulting from the incorporation of the PC within the waveguide) has been used[14]. The model allowed the calculation of coupling coefficients κ_1 and κ_3 between both in-plane propagating and orthogonal waves in a PCSEL. However, models based on coupled-mode theory are difficult to use, and they need to be developed for each PC lattice type and polarisation of waves. On the other hand, finite-difference time-domain solvers[11] are time and computer memory demanding, a FDTD model of a PCSEL developed for a PCSEL with a PC can be applied to PCSELs with PCs of other geometries. These models account for most of the physical effects (diffraction, reflection, waveguiding etc.), rely on minimal assumptions, and allow calculations of far fields.

In this work, we use a FDTD solver[11] and an eigenmode solver[12] to investigate band diagrams of bulk PCs, PC layers, and PCSELs. We also calculate diffraction loss and surface emission power of PCSELs. These calculations have been done assuming that the PCSEL has translation symmetry. This implies that instead of simulating the entire PCSEL, we can simulate one unit cell of the PCSEL by applying Bloch periodic boundary conditions at boundaries along translation directions (X and Y) and performing simulations at Γ point of the photonic band diagram only. There is no periodicity along the Z direction, and, thus, absorbers are placed near boundaries to absorb waves propagating towards and away from these boundaries. Application of absorbers rather than perfectly matched layers made the calculation of both diffraction loss and spectrum of surface emission possible, improving the convergence.

There is another family of modelling tasks such as the calculation of far fields that requires the entire structure to be simulated to allow interference of surface emitted waves and the formation of diffracted beams. In such cases the entire PCSEL structure has been simulated, but this has been carried out with a lower FDTD mesh density to reduce memory demands.

A dipole point source used in the simulation is situated inside the active zone; it generates TE-polarised waves, and has a Gaussian intensity spectrum. Its emission maximum is centred at 960 nm and its spectral linewidth matches the linewidth of the PL emission spectrum of PCSELs[7]. The source operates for a period of time derived by the source linewidth. As it stops operating, waves with frequencies corresponding to resonant modes continue oscillating and form standing waves (modes) in the laser cavity. The point detector is situated inside the active zone collecting data to extract mode properties such as their frequencies and Q-factors. The other group of detectors measures power flux spectra of their in-plane propagating waves, for upwards and downward emission.

4. RESULTS

4.1 Convergence study

In this work, we are mostly interested in the power of surface emission and the frequency of modes. Thus, convergence studies of the real part of the mode frequency and the power of surface flux both versus the mesh resolution of the FDTD method have been carried out. The mesh resolution is the number of FDTD mesh nodes per PC period. Fig. 2 shows the steady state error versus the resolution assuming that the steady state corresponds to a resolution of 150.

When the model is applied to PCSELs with PCs of either type I or II, the steady state error in calculation frequency is less than □1% for a mesh resolution exceeding 20. However, the dependence of the steady-state error of surface flux suggests that the error lies within □1% range for mesh resolutions exceeding 100. Further increasing the mesh resolution does not improve results in any way, but raises the calculation time and computer memory required.

Thus, the results shown in this report are calculated for a mesh resolution of 100 which corresponds to the optimum balance between good convergence and the calculation time.

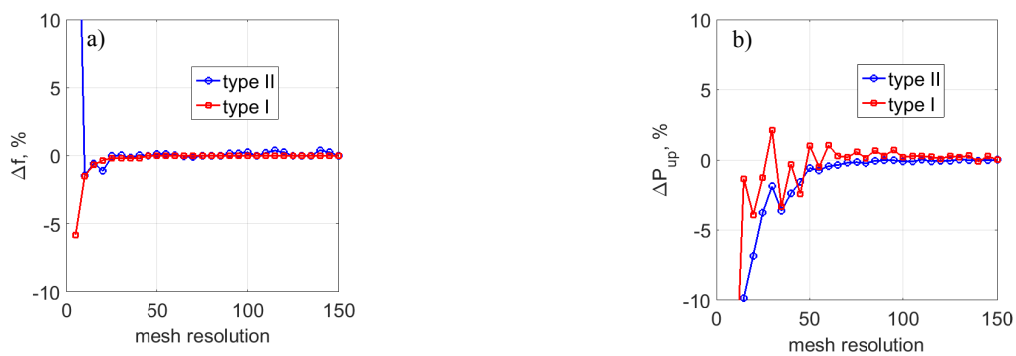

Figure 2. (a) steady-state error of real part of mode frequency versus the resolution and (b) the steady-state error of surface power flux versus the resolution. r/a=0.35 unless otherwise stated.

4.2 Band diagrams of bulk PC

Before applying the FDTD model to a PCSEL, we first compare FDTD results to results of the standard eigemode solver[12]. In this case, Bloch periodic boundary conditions are applied to all boundaries of the three-dimensional model of the two-dimensional photonic crystal of type II nature. Fig. 3a shows the photonic band diagram of the PC at the Γ point calculated using the eigenmode solver[12]. There are 4 bands (modes) at this point of the diagram, two of them, namely C and D are degenerate. Fig. 3b shows the dependence of frequencies of these bands on the r/a ratio of the PC overlaid with the surface power flux spectrum calculated using the FDTD method. Results of these two methods are in excellent agreement. Band A provides the highest power flux in the spectrum. At r/a=0.3, the bands intersect and single-mode radiation is observed. Table 1 shows the time-averaged electric-field energy density of bands A, B, C and D. Bands C and D, as well as in type I PC, have periodic electric field distribution, their electric field can interfere constructively and this results in surface emission.

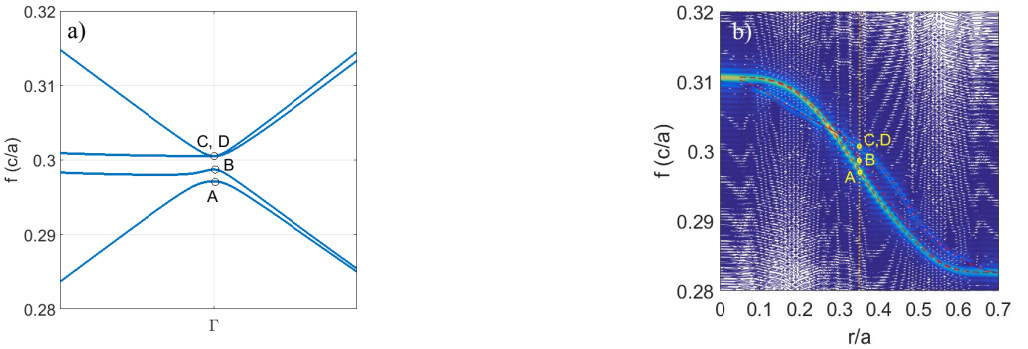

Figure 3. (a) band diagram of PC type II at r/a=0.35 (eigenmode solver result) and (b) band diagrams (eigenmode solver) overlaid on power flux across PC atoms (FDTD solver result). The vertical line in (b) corresponds to r/a=0.35.

Table 1. Time-averaged electric-field energy density ($\varepsilon |E|^2$) of two-dimensional PC type II calculated using eigensolver.

r/a	Band A	B	C	D
0.2	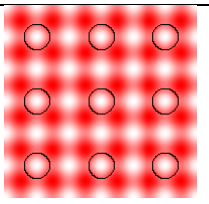	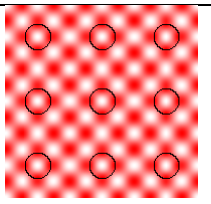	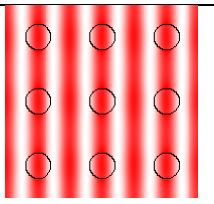	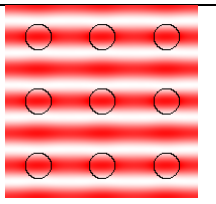
0.35	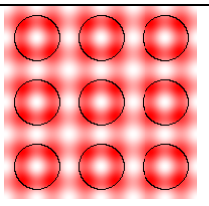	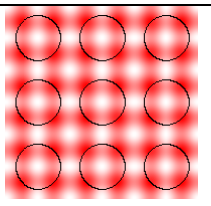	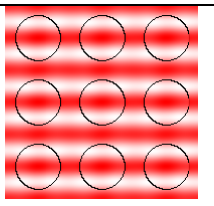	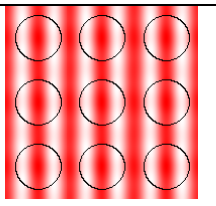

Fig. 4 shows the surface power flux of a membrane layer of the PC and the PCSEL. The membrane PC layer has a thickness of 150 nm, the same as the PC layer used in PCSELs. It sits inside GaAs as it does in the PCSELs. The characteristic shows that frequencies of bands are shifted to lower frequencies in the membrane and that band A has the highest intensity. Fig. 4b shows that this mode appears in the spectrum of the PCSEL. The dashed line is the frequency of the mode calculated using the FDTD method. The in-plane power of the mode grows in the r/a range from 0 to 0.15, and then drops at 0.3. It grows again as r/a increases further. This behaviour is similar to the case for a DFB lasers with a second-order grating[15], and the mode in the PCSEL demonstrates DFB-like behaviour and peaks optical feedback at r/a=0.2 and r/a>0.3. It worth noting, that simplified models based on a coupled mode theory also suggested a maximum of in-plane feedback and coupling at these r/a ratios.

Fig. 5a shows the diffraction loss of the PC mode registered by detector planes of the FDTD solver in far-field region and Fig. 5b shows the normalised surface power flux. Calculated diffraction losses in limit of r/a from 0 to 0.1 are not reliable because the FDTD model suffers from high mesh errors as Fig. 4b shows. However, at r/a=0.2 the diffraction loss reaches a maximum of 40-65 cm^{-1}. The PCSEL should emit at this r/a ratio and Fig. 5b shows that it is exactly what happens. Surface emission drops at r/a>0.2. A closer analysis shows that the dependence of Q factor of the mode on the r/a has a lower Q at r/a=0.2 whilst in-plane intensity of the mode is high as Fig. 4b shows. This lowering of Q factor can only be explained by high orthogonal scattering of waves from atoms resulting in surface emission at r/a=0.2. The maximum emission at r/a=0.2 is also suggested by modelling results[14] based upon couple-mode theory[9]. They have shown that the product of coupling factors of in-plane and orthogonal cooling has a maximum at r/a=0.2-0.25, thus the PC provides maximum feedback and yet high surface emission under this condition.

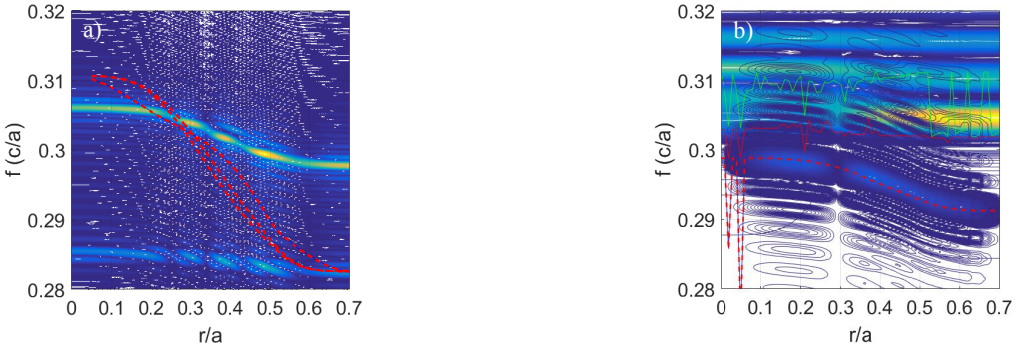

Figure 4. (a) frequency bands of bulk PC type II overlaid on the surface flux spectrum of the PC membrane layer and (b) frequency bands of PCSEL overlaid on the flux spectrum measured across the laser waveguide(in-plane propagation), all calculated using FDTD method.

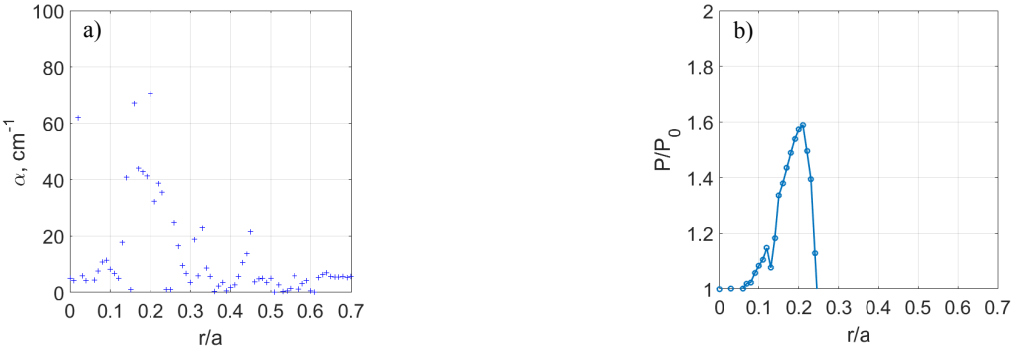

Figure 5. (a) radiation loss of the PC mode in PCSEL and (b) normalised surface flux of spectral maximum measured above the PCSEL in far-field region. Red solid line in (a) is a fitting line. Both dependencies are calculated using FDTD model of the PCSEL.

5. CONCLUSION

In this work we have utilised three-dimensional FDTD models to investigate two-dimensional bulk PCs, PC layers embedded in GaAs, and all-semiconductor PCSEL structures to explore PCSEL characteristics. Although FDTD models are time and computer memory demanding, they allow the investigation of PCSEL characteristics in a direct way, without using a complex theory (such as couple-mode theory of a PC), can model the entire PCSEL including all its waveguide layers, and can calculate mode profiles, their resonance wavelengths and diffraction losses resulting from the incorporation of the PC with the laser. The only significant assumption of the model is periodicity of the structure. This assumption is made in order to reduce time and memory demands of the model, and improve the convergence of the method. We consider that this can be considered as a valid assumption keeping in mind that the PCSEL itself is 500 PC periods long in each direction, and that typical coupling coefficients are ~3000 cm^{-1}, corresponding to ~0.1 per PC period.

In has been shown in this report that results of the FDTD model and the eigenmode solver applied to a two-dimensional PC are in excellent agreement. Thus, the model has been applied to both a PC membrane encapsulated within GaAs, and the full PCSEL. Results have shown that the PCSEL reaches its surface emission maximum at r/a=0.2, where the radiation loss of the PCSEL reaches 40-60 cm^{-1}. Radiation loss of the laser without the PC is about 5 cm^{-1}, thus, diffraction loss is in the range from 35 to 55 cm^{-1}. Such high diffraction loss should raise the threshold gain by a factor of two as compared to the structure with the PC removed. The emission maximum at r/a=0.2 is a combined result of two effects: maximum in-plane coupling (κ_3) and high out of plane scattering that lowers the Q factor of the cavity.

6. REFERENCES

[1] Yokoyama, M. and Noda, S., "Polarization Mode Control of Two-dimensional photonic crystal laser having a square lattice structure," IEEE Quant. Electron., 39(9), 1074-1080 (2003).

[2] Hirose, K., Liang, Y., Kurosaka, Y., Watanabe, A., Sugiyama, T. and Noda, S., "Watt-class high-power, high-beam-quality photonic-crystal lasers," Nature Photonics, 8, 406–411 (2014).

[3] Kurosaka, Y., Sakai, K., Miyai, E. and Noda, S., "Controlling vertical optical confinement in two-dimensional surface-emitting photonic-crystal lasers by shape of air holes," Optics Express 16(22), 18485–18494 (2008).

[4] Liang, Y., Peng, C., Sakai, K., Iwahashi, S. and Noda, S., "Three-dimensional coupled-wave model for square-lattice photonic crystals with transverse electric polarization: a general approach," Phys. Rev. B 84, 195119 (2011).

[5] Taylor, R. J. E., Childs, D. T. D., Ivanov, P., Ben J. Stevens, Babazadeh, N., Sarma, J., Khamas, S., Crombie, A. J., Li, G., Ternent, G., Thoms, S., Zhou, H. and Hogg, R. A., "Coherently coupled photonic-crystal surface-emitting laser array," IEEE Sel. Topics in Quant. Electron. 21(6), 4900307–4900307 (2015).

[6] Taylor R. J. E., Childs D. T. D., Ivanov P., Stevens B. J., Babazadeh N., Crombie A. J., Ternent G., Thoms S., Zhou H. and Hogg R. A., "Electronic control of coherence in a two-dimensional array of photonic crystal surface emitting lasers," Scientific Reports 5, 13203 (2015).

[7] Williams, D. M., Groom, K. M., Stevens, B. J., Childs, D. T. D., Taylor, R. J. E., Khamas, S., Hogg, R. A., Ikeda, N. and Sugimoto. Y., "Epitaxially regrown GaAs-based photonic crystal surface-emitting laser," Photonics Technology Letters 24(11), 966–968 (2012).

[8] Peng, C., Liang, Y., Sakai, K., Iwahashi, S. and Noda, S., "Coupled-wave analysis for photonic-crystal surface-emitting lasers on air holes with arbitrary sidewalls," Optics Express 19(24), 24672–24686 (2011).

[9] Sakai, K., Miyai, E. and Noda, S., "Coupled-wave model for square-lattice two-dimensional photonic crystal with transverse-electric-like mode," Appl. Phys. Lett. 89(2), 021101 (2006).

[10] Sakai, K., Miyai, E. and Noda, S., "Two-dimensional coupled wave theory for square lattice photonic crystal lasers with TM-polarization," Opt. Express, 15(7), 3981–3990 (2007).

[11] Oskooi, A. F., Roundy, D., Ibanescu, M., Bermel, P., Joannopoulos, J. D. and Johnson, S. G., "MEEP: A flexible free-software package for electromagnetic simulations by the FDTD method," Computer Physics Communications 181(3), 687–702 (2010).

[12] Johnson, S. G. and Joannopoulos J. D., "Block-iterative frequency-domain methods for Maxwell's equations in a planewave basis," Optics Express 8(3), 173–190 (2001).

[13] Taylor, R. J. E., Williams, D. M., Orchard, J. R., Childs, D. T. D., Khamas, S. and Hogg, R. A., "Band structure and waveguide modelling of epitaxially regrown photonic crystal surface-emitting lasers," J. Phys. D: Appl. Phys. 46(26), 264005 (2013).

[14] Ivanov, P., Taylor, R. J. E., Crombie, A., Childs, D. T. D., Khamas, S., Sarma, J. and Hogg, R. A., "Waveguide and photonic crystal design of photonic crystal surface-emitting laser," Proc. SPIE 9382, 93821A, (2015).

[15] Ghafouri-Shiraz, H., [Distributed Feedback Laser Diodes and Optical Tunable Filters], John Wiley & Sons, 75 (2003).